NMR Screening for Lead Compounds Using Tryptophan-Mutated Proteins

Ulli Rothweiler,[†] Anna Czarna,[†] Lutz Weber,[‡] Grzegorz M. Popowicz,[†] Kinga Brongel,[†] Kaja Kowalska,[†] Michael Orth,[†] Olaf Stemmann,[†] and Tad A. Holak*,[†]

Max Planck Institute for Biochemistry, D-82152 Martinsried, Germany, NexusPharma Inc., 253-13 Summit Square Center, Langhorne, Pennsylvania 19047-1098

Received March 14, 2008

NMR-based drug screening methods provide the most reliable characterization of binding propensities of ligands to their target proteins. They are, however, one of the least effective methods in terms of the amount of protein required and the time needed for acquiring an NMR experiment. We show here that the introduction of tryptophan to proteins permits rapid screening by monitoring a simple 1D proton NMR signal of the NH side chain ($^{N}H^{\varepsilon}$) of the tryptophan. The method could also provide quantitative characterization of the antagonist−protein and antagonist−protein−protein interactions in the form of K_Ds and fractions of the released proteins from their mutual binding. We illustrate the method with the lead compounds that block the Mdm2−p53 interaction and by studying inhibitors that bind to cyclin-dependent kinase 2 (CDK2).

Introduction

NMR-based drug screening methods, in particular the NMR chemical shift perturbation method, are powerful techniques used for the identification and characterization of ligand−protein interactions.[1–7] The now widely used screening approach "SAR by NMR" employs typically ^{15}N-labeled proteins that are monitored by 2D ^{15}N−^{1}H-correlation NMR spectroscopy.[1,2] Approximately 2 mg of protein (0.5 mL of a 0.2 mM solution)[1,2,8] are required for a 15 kDa protein per tested ligand or mixture of ligands. Lower concentrations of protein can be used, but this goes with the expense of the time needed to record a qualitatively acceptable spectrum. The microcoil-probe NMR technology, enhanced with the cryoprobe detection, can help in lowering the amount of protein needed to microgram quantities,[9] but still the performance of NMR is "slow" compared to other high-throughput techniques like, for example, fluorescence spectroscopy.[10*a*]

We show here that simple 1D proton NMR spectra on unlabeled proteins (i.e., no ^{15}N or ^{13}C labeling required) can be utilized in screening for lead compounds and thus permitting rapid ligand characterization. Because signal overlap in proton 1D spectra of proteins may present a problem, one must have or must introduce an amino acid "reporter" that has at least one nonoverlapped NMR signal that is sensitive to the binding of a ligand to the investigated protein. We have chosen to introduce tryptophan; this is because it is the only amino acid whose NH indole side chain ($^{N}H^{\varepsilon}$) gives an NMR signal at around 10 ppm at physiological pH; the signal is hence well separated from the bulk of amide protons and can be easily monitored.[11]

We have recently described a two-dimensional ^{15}N-HSQC-based NMR assay for studying the effect of antagonists on protein−protein interactions.[12,13] The method, named AIDA (for antagonist induced dissociation assay), provides information on whether an antagonist of a protein−protein interaction is strong enough to dissociate the complex and whether its action is through denaturation, precipitation, or release of a protein in its functional folded state. AIDA requires a large protein fragment (larger than 30 kDa) to bind to a small reporter protein (less than 20 kDa). By using extra tryptophan-bearing proteins, we show here that a 1D proton NMR version of AIDA-NMR can be used universally in competition experiments for monitoring ligand/protein−protein complexes. In addition, we have studied binary interactions between ligands and target proteins with 1D NMR using the same tryptophan mutants.

We illustrate our method on the p53−Mdm2 interaction[14–26] and on inhibitors of cyclin-dependent kinase 2 (CDK2). The tumor suppressor p53 protein, "the guardian of the genome", has an overarching role in protecting the organism from cancer.[14–26] It regulates, as a potent transcription factor, many downstream genes involved in the cell cycle control, antiangiogenesis, and apoptosis. To escape the "safeguard" system mediated by p53, nearly all human cancers have either mutated the p53 itself (50% all cancers) or compromised the effectiveness of the p53 pathway. In tumors that retain the wildtype p53, the p53 pathway is mostly inactivated by its negative regulator, the Mdm2 protein—a principal cellular antagonist of p53. Mdm2 interacts through its ca. 118-residue amino terminal domain with the N-terminal transactivation domain of p53.[14–16,19,20] In several recent studies, it was shown that the disruption of the p53−Mdm2 interaction or the suppression of the Mdm2 expression can activate the p53 pathway and inhibit tumor growth.[24–26] Thus the restoration of the impaired function of a single gene, p53, by disrupting the p53−Mdm2 interaction in cancers that still are endued with the wildtype p53, offers a profoundly new avenue for anticancer therapy across a broad spectrum of cancers.[14,17,18,23–26] Several low-molecular-weight compounds have been reported that bind to Mdm2 (refs 15, 16, 26–32). The best-documented drug-like compounds developed are *cis*-imidazoline derivatives called nutlins (Figure 1).[26] Nutlin-3 is a selective and potent inhibitor of the p53−Mdm2 interaction, which induces apoptosis in p53 wild type cells and shows in vivo efficacy in mice xenograft models.

The passage of the cell through different phases (G1 → S → G2 → M) of the cell cycle is controlled by cyclins and their associated cyclin-dependent kinases (CDKs).[33,34] In the G1

* To whom correspondence should be addressed. Phone: (+49) 89-8578-2673. Fax: (+49) 89-8578-3777. E-mail: holak@biochem.mpg.de.
† Max Planck Institute for Biochemistry.
‡ NexusPharma Inc.

a Abbreviations: AIDA, antagonist induced dissociation assay; GST, glutathione *S*-transferase; Mdm2, murine double minute 2; CDK2, cyclin-dependent kinase 2; p53(1−310), a domain of human p53 between residues 1−310; HSQC, heteronuclear single quantum coherence; ITC, isothermal titration calorimetry.

10.1021/jm8002813 CCC: $40.75
Published on Web 08/05/2008

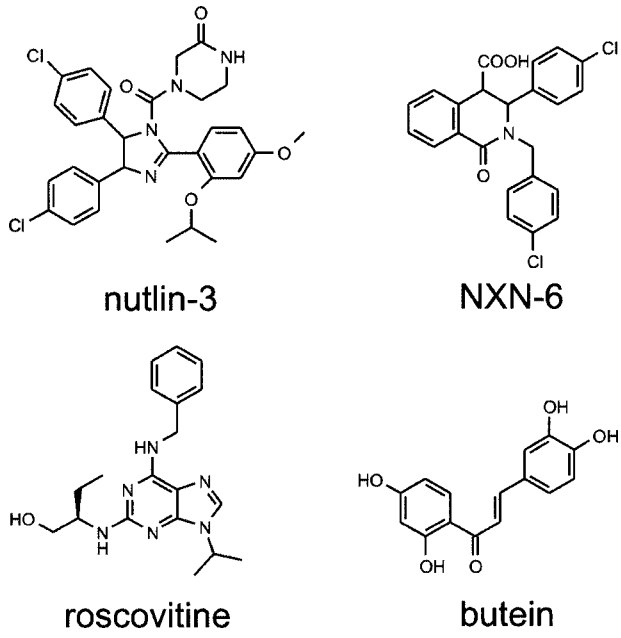

Figure 1. Inhibitors for Mdm2 and CDK2.

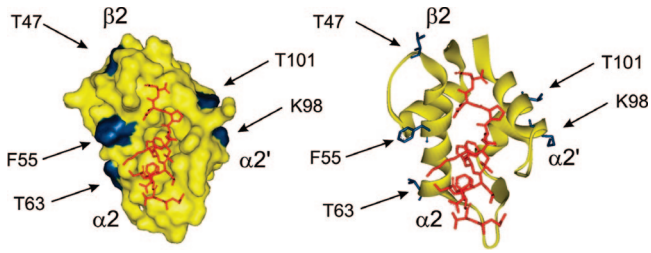

Figure 2. Surface and ribbon plots of human Mdm2 bound to a p53 peptide.[48] Mutated amino acids are shown in blue, the p53 peptide is shown in red.

phase, the activated CDKs phosphorylate the retinoblastoma protein (pRb) and turn off its transcriptional suppressor activity.[35–37] As a result, the activation of a set of genes required for entry into S phase, including cyclin E, is enhanced. Cyclin E activates CDK2 in late G1 phase and irreversibly commits the cell to the cell division and transition into S phase through hyperphosphorylation pRb.[38,39] This commitment is also active in tumor cells; thus inhibiting CDKs should in principle arrest or stop the progression of the uncontrolled tumor cell division. A number of CDK inhibitors of considerably different chemical classes have been reported.[40,41] For CDK2, one extensively tested inhibitor is roscovitine (seliciclib, CYC202) (Figure 1).[42–45] Roscovitine is an orally bioavailable compound with high selectivity for CDK1, 2, 7, and 9 (ref 40). Preclinical studies have shown antitumor effects in a broad number of human tumor xenografts,[44–47] and phase I clinical trials are ongoing.[47]

Results

Design of Tryptophan Mutants of Mdm2. The human wild type Mdm2 protein (wt-Mdm2) does not have any tryptophans within its first 118 residues. Several mutations were therefore selected for residues that were close to the binding pocket for p53 but would be expected not alter this site. The mutated residues are part of the α2 (F55W and T63W), α2′ (K98W and T101W) helices, and for the T47W mutation of the β2 strand (Figure 2).[48] Their side chains point into the solvent, in the opposite direction to the binding pocket, and they seem to not have steric clashes with the rest of the protein. They should therefore exhibit a considerable freedom of motion.

One-dimensional proton NMR spectra of T47W, F55W, T63W, K98W, and T101W were almost identical to that of the wt-Mdm2 spectra (with the exception of an extra signal at around 10 ppm, which originates from $^{N}H^{\varepsilon}$ of the newly introduced tryptophan). This indicated that the mutated Mdm2 constructs were correctly folded (Supporting Information Figure S1). Protein melting analysis showed that the mutants have similar midpoint of thermal transition (melting temperature), indicating that the changes in their stability against denaturation were insignificant; in fact, the F55W, T101W, and K98W mutants were slightly more temperature stable than wt-Mdm2 (Supporting Information Figure S2).

An Antagonist Induced Dissociation Assay (AIDA) for Targeting Protein−Protein Interactions in 1D NMR Competition Binding Experiments. The N-terminal domain of p53 (residues 1−73) has two tryptophan residues and we have used 1D proton spectra of the $^{N}H^{\varepsilon}$ side chains of these tryptophan residues for monitoring the state of p53 in Mdm2/GST-p53 (residues 1−73) complexes upon treatment with various ligands. Figure 3 (top traces) shows NMR spectra of the tryptophan residues of the free, Mdm2-unbound p53. Because of a highly flexible nature of the N-terminal domain of p53, the side chains of W23 and W53 give rise to sharp lines.[12,13,49]

On forming the complex with wt-Mdm2, the signal of W23 disappears (Figure 3, middle spectra). This is because W23, together with the p53 residues 17−26, comprise the primary binding site for Mdm2. Upon binding, these residues participate in well-defined structures of large p53-Mdm2 complexes, whereas W53 is still not structured when p53 is bound to Mdm2 (refs 12, 49). The observed $1/T_2$ transverse relaxation rate of the bound W23 in the complexes increases thus significantly and broadening of NMR resonances results in the disappearance of this signal in the spectra.[12,13,49]

Nutlin-3 was then added to the Mdm2/p53 complex. The chemical formula of nutlin-3 and other used inhibitors is given in Figure 1. For nutlin-3, the W23 peak reappears and the NMR spectrum indicates a complete p53 release (Figure 3a, bottom spectrum). The NMR spectrum additionally showed that the Mdm2/nutlin-3 complex is soluble and that nutlin-3 did not induce precipitation of Mdm2. Similar results were obtained for NXN-6 (*trans*-2-(4-chlorobenzyl)-3-(4-chlorophenyl)-1-oxo-1,2,3,4-tetrahydroisoquinoline-4 carboxylic acid).[50,51] This compound, however, is not as efficient as nutlin and was capable to release ca. 70% of p53 (Figure 3b, bottom spectrum).[51]

We have shown above that for the p53-Mdm2 interaction, we can use 1D proton NMR spectra of the Trp $^{N}H^{\varepsilon}$ of p53 for monitoring the p53-Mdm2 complex and p53 itself upon treatment with ligands. In general, however, the highly flexible nature of the N-terminal domain of p53 is an exception rather than a rule.[12,13,49] (see also the Discussion section below). With the tryptophan Mdm2 mutants, we have universal reporters for monitoring the complexes through the $^{N}H^{\varepsilon}$ NMR signals. For a specific case of the p53−Mdm2 interaction, we can now monitor directly the status of the p53−Mdm2 complex, the Mdm2 binding to p53 and of p53 to Mdm2.

Figure 4a shows the spectrum of the complex of Mdm2−T47W with p53 (residues 1−73). The $W23^{p53}$ signal disappeared, indicating the complex formation; the $47W^{Mdm2}$ is broadened, while the $W53^{p53}$ is unaffected. Addition of nutlin-3 fully dissociates the complex as seen by the recovery of full intensities for the $47W^{Mdm2}$ and $W23^{p53}$ tryptophan NMR signals (Figure 4b). Similar results were obtained for the titration of the complex

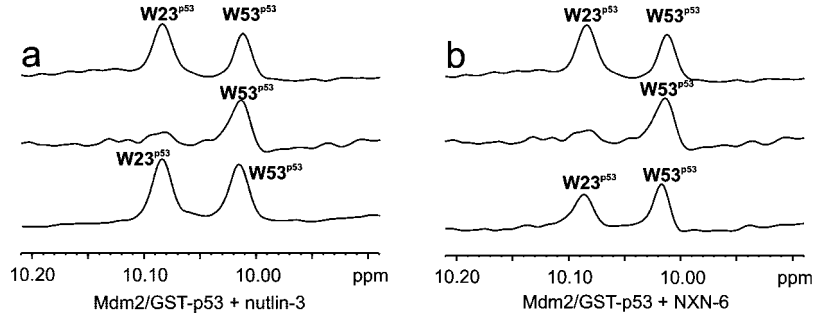

Figure 3. NMR competition binding experiments. (a) Titration of wt-Mdm2/p53 with nutlin-3. One-dimensional proton spectrum of the side chains of tryptophans (W) of free p53 (residues 1−73), showing W23, W53 (upper trace). On forming a complex with wt-Mdm2, the signal of the side chain of W23 disappears (middle trace). After addition of nutlin-3, the signal of W23 is recovered as a result of a complete dissociation of the p53/Mdm2 complex (lower spectrum). (b) Titration of wt-Mdm2/p53 with NXN-6. Upper and middle spectra are the same as for wt-Mdm2-p53 and nutlin. After addition of NXN-6, the recovery of the W23 signal is about 70% in the lower spectrum.

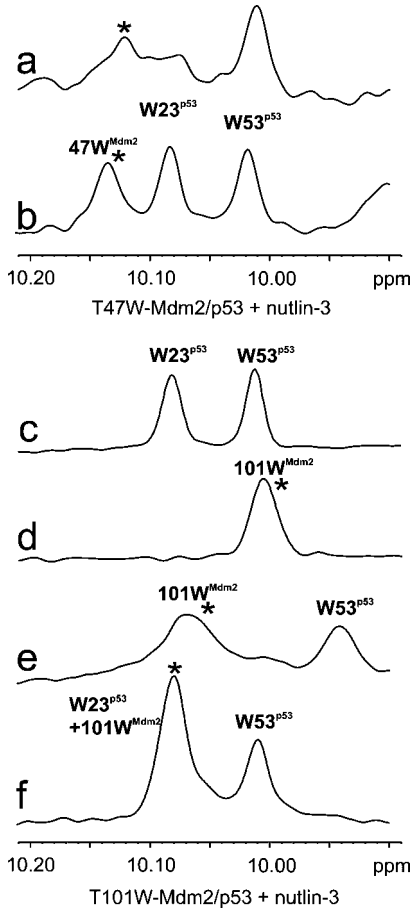

Figure 4. Titration of the complexes GST-p53 (residues 1−73)/Mdm2-T47W (a,b) and GST-p53/Mdm2-T101W (c−f) with nutlin-3. (a) Spectrum of the GST-p53/Mdm2-T47W complex. (b) After addition of nutlin-3, the two protein complex components are freed and three, well-resolved tryptophan signals (47W from Mdm2 and W23 and W53 from p53) are seen. (c) 1D proton spectrum of the side chains of tryptophans (W) of free p53, showing W23, W53. (d) 1D proton spectrum of the free, unbound Mdm2−T101W, showing 101W. (e) The spectrum of GST−p53/Mdm2−T101W complex. (f) After addition of nutlin-3, the complex is dissociated and the two proteins are separated. By coincidence the signal of $101W^{Mdm2}$ of the nutlin-bound Mdm2−T101W appears at the same position as W23 of p53 at around 10.1 ppm.

between p53 and Mdm2−T101W (Figure 4c−f). The free p53 (residues 1−73) is shown in Figure 4c, the free, unbound Mdm2−T101W is shown in Figure 4d. Figure 4e shows the proton $^{N}H^{\varepsilon}$ signals of the complex. The signal of the p53 bound

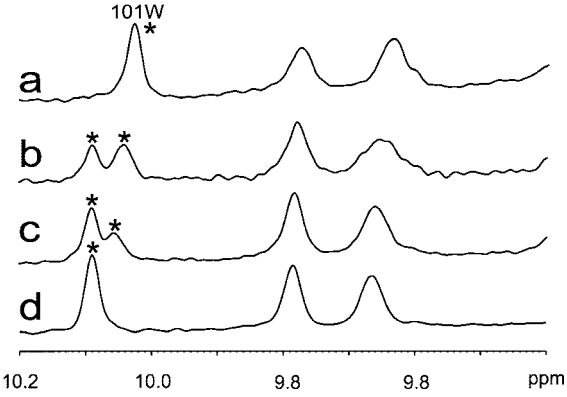

Figure 5. One-dimensional proton NMR spectra of human Mdm2−T101W titrated with nutlin-3. (a) Unbound Mdm2. (b) Molar ratio of the protein:inhibitor 1:0.5. (c) Molar ratio protein:inhibitor 1:0.75. (d) Molar ratio protein:inhibitor 1:1.

$101W^{Mdm2}$ is shifted downfield compared to that of the free Mdm2−T101W and is now at the position of free $W23^{p53}$. After addition of nutlin-3 (Figure 4f), the signal of the nutlin-bound $101W^{Mdm2}$ is shifted to the position seen in (Figure 5) and coincides with the signal of freed $W23^{p53}$. Summation of both signals $101W^{Mdm2}$ and $W23^{p53}$ indicates that p53 is 100% released and Mdm2-unbound. NMR spectra clearly show that indole side chains of Trp's in the mutants are flexible; the line width ($\Delta\nu_{exp}$) is in the range of 14 ± 1 Hz, whereas the $\Delta\nu_{exp}$ of a few resolved backbone amides is 25 ± 5 Hz. Mutant Trp's get restricted in motions only upon binding to p53 (Figures 4, 5a, 6a, and Supporting Information Figure S3).

Similar results were obtained for the F55W−Mdm2 mutant when its p53/Mdm2 complex was titrated with nutlin-3 and NXN-6 (Supporting Information Figure S3). The $55W^{Mdm2}$ NMR signal of the Mdm2−F55W/p53 complex comes at an almost identical position as the signal of W23 of p53. The release of p53, after addition of nutlin-3, is therefore indicated by an increase of the signal at 10.0 ppm, which is the summation of $55W^{Mdm2}$ and $W53^{p53}$, while the release of p53 after addition of NXN-6 is indicated by an increase of the signal at 10.1 ppm, which is the summation of $55W^{Mdm2}$ and $W23^{p53}$. These titrations showed a complete p53 release after an excess addition of nutlin-3; for NXN this release was 70%.

The Binary Interaction of Ligands with Target Proteins (Mdm2). All mutated Mdm2 constructs were also tested for their binary binding to ligands. We started with nutlin-3. Nutlin-3 binds tightly to human wild type Mdm2 with affinity of 0.7 μM (for the nutlin racemic mixture)[12,26,49] and in NMR

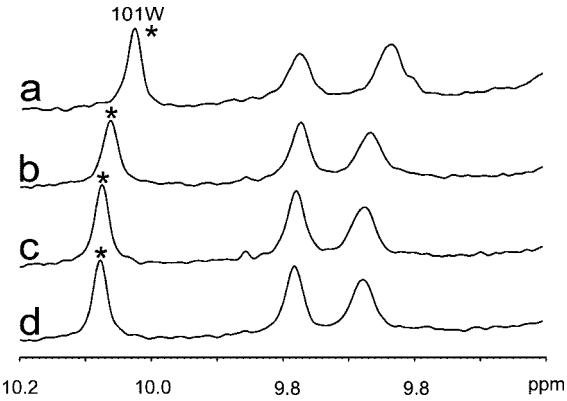

Figure 6. One-dimensional proton NMR spectra of human Mdm2−T101W titrated with NXN-6. (a) Unbound Mdm2. (b) The molar ratio protein: inhibitor 1:0.5. (c) The molar ratio protein:inhibitor 1:0.75. (d) Molar ratio protein: inhibitor 1:2.

Table 1. ITC and NMR Titration Data for Mdm2 Mutants[a]

	Mdm2	T101W	K98W	F55W
GST-p53	0.50 ± 0.05	0.47 ± 0.09		
nutlin-3	0.70 ± 0.08[b]	<1[c]; <0.5[d]	<1[c]; <0.5[d]	<0.5[c]
NXN-6	2 ± 2; 8 ± 2[c]; 2 ± 2[d]	3 ± 1[c]		9 ± 4[c]; 3 ± 2[d]

[a] K_Ds (μM) determined by ITC unless indicated otherwise. [b] K_D in μM from ref 52. [c] K_Ds (μM) determined by the NMR ligand-protein binary titration. [d] K_Ds (μM) obtained from the AIDA experiment.

^{15}N-HSQC experiments shows classical characteristics of slow chemical exchange between nutlin-bound and free Mmd2s (ref 12). Figure 5 shows the nutlin−Mdm2 1D NMR titration using the T101W mutant. At a molar ratio of protein/nutlin of 1:0.5, we could observe two signals for 101W: one at the same position as the starting peak, the second shifted downfield by 0.1 ppm. Both signals have intensities that are half of the size of the starting signal with no nutlin-3 present. This indicates that we have two species, a free T101W mutant and a complex made of T101W and nutlin-3 that interchange slowly on the NMR time scale.[11] At a concentration of 1:1, only one peak can be detected at the position of the complex, while the peak of the free 101W completely disappeared (Figure 5d). The K98W mutant gave similar results. Titrations for both mutants indicated K_D's below 1 μM for the interaction between nutlin-3 and Mdm2, in excellent agreement with the 0.7 μM K_D wildtype Mdm2 data.[26,52]

The F55W mutant did not show any changes in the position of the tryptophan side chain in the proton NMR spectrum upon adding increasing amounts of nutlin-3. The T47W and T63W mutants showed induced chemical shifts upon titrating with nutlin-3; however, the difference between NMR chemical shifts of the tryptophan NMR signal of the fully nutlin-bound Mdm2 and that of free Mmd2 were 0.009 and 0.022 ppm, respectively. This is too close for resolving the peaks corresponding to these two species at intermediate steps of titrations.

We next tested a recently developed inhibitor of the Mdm2/p53 interaction:[50,51] a compound called NXN-6, for which isothermal titration calorimetry (ITC) indicated binding to Mdm2 at the K_D of 2 μM (Table 1). Stepwise titration of T101W with NXN-6 showed that the tryptophan signal did not split but continuously moved from the starting point toward the end point of the titration (Figure 6).

The movement of the averaged peak showed that NXN-6 is in fast exchange with the protein.[11,12] The NMR titration of Figure 6 produced the K_D of 3 μM, in excellent agreement with the ITC data for wt-Mdm2 in Table 1. An interesting difference between nutlin-3 and NXN-6 was seen for titrations with the

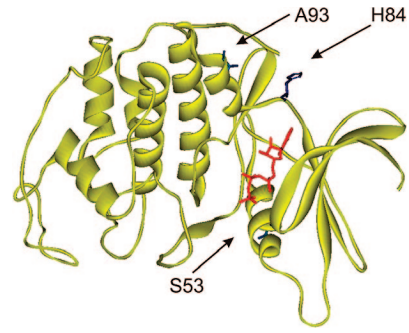

Figure 7. Ribbon plot of CDK2. The mutated amino acids are shown in blue; the bound ATP is shown in red.[53]

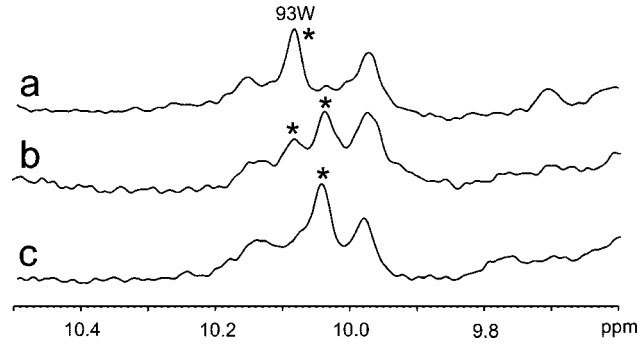

Figure 8. One-dimensional NMR spectra of human CDK2−A93W titrated with roscovitine. (a) Unbound CDK2. (b) Molar ratio protein: inhibitor 1:0.6. (c) Molar ratio protein: inhibitor 1:1. The asterisk indicates the newly introduced tryptophan 93W.

F55W mutant. Although nutlin-3 did not induce any chemical shift perturbations in the $^{N}H^{\varepsilon}$ tryptophan region of NMR spectra, the $^{N}H^{\varepsilon}$ tryptophan NMR signal was sensitive to the titration with NXN-6, showed a continuous movement of the tryptophan signal comparable to that of T101W seen in Figure 6, and indicated the K_D of 9 μM (Table 1).

The Binary Interaction of Ligands with CDK2. In contrast to Mdm2, the full-length CDK2 protein has four endogenous tryptophans within its amino acid sequence. Because CDK2 is three times larger than the N-terminal domain of Mdm2, the tryptophans, which are all buried inside the molecule, give rise to broadened NMR signals and, although well separated from each other, they were not sensitive to the binding of inhibitors that we tested. Other regions of the CDK2 spectrum could also not provide unambiguous conclusions on ligand bindings (Supporting Information Figure S4).

We chose three point mutants for CDK2 based on the considerations made for Mdm2. The mutants are shown in Figure 7.

Similarly to Mdm2 mutants, the CDK2 mutants gave almost identical NMR spectra compared to that of the wild type (Supporting Information Figure S5) and their melting points were almost identical at around 40 °C (Supporting Information Figure S6). The NMR spectra showed also that the indole side chains of the introduced Trp is flexible, with the line width ($\Delta\nu_{exp}$) of 19 ± 2 Hz, whereas the $\Delta\nu_{exp}$ of the NH indole of native Trp′s is 29 ± 4 Hz and the estimated $\Delta\nu_{exp}$ of backbone amides between 50−60 Hz (Figures 810, Supporting Information Figure S5).

For the S53W mutant, the signal was broadened and weak, and the H84W and the A93W mutant gave sharp signals. The newly introduced tryptophan of the H84W mutant overlaps with one endogenous tryptophan, whereas the signal of the tryptophan

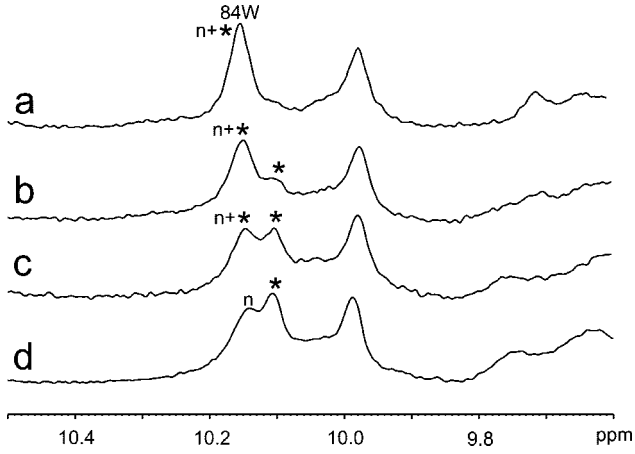

Figure 9. One-dimensional proton NMR spectra of human CDK2−H84W titrated with roscovitine. (a) Free CDK2. (b) The molar ratio protein: inhibitor, 1:0.3. (c) Molar ratio protein:inhibitor, 1:0.6. (d) Molar ratio protein:inhibitor, 1:1. The asterisk indicates the new introduced tryptophan 84W, the endogenous tryptophan is marked with a small n.

of the A93W mutant was well separated from the rest of the $^{N}H^{\varepsilon}$ Trp signals (Supporting Information Figure S5). We first titrated the A93W mutant with roscovitine (Seliciclib, CYC202). Roscovitine is a strong binding CDK2 inhibitor with an IC_{50} of 0.1 μM (for chemical formulas, see Figure 1).[45] A stepwise addition of roscovitine leads to a splitting of the new tryptophan, indicating strong binding (Figure 8).

Identical behavior was seen in titrating the H84W mutant with roscovitine (Figure 9). Because of the overlap with the endogenous peak at around 10.15 ppm, the starting peak is a sum of 84W and an endogenous tryptophan.

We next tested a weak inhibitor for CDK2. Butein (3,4,2′,4′-tetrahydroxychalone), a plant polyphenol, was first described as a novel cAMP-specific phosphodiesterase inhibitor, which produced endothelium dependent relaxation of rat aorta.[54] It inhibits the tyrosine specific protein kinases, like the EGF receptor tyrosine kinase and $p60^{c\text{-}src}$ with an IC_{50} of 16 μM and 65 μM, respectively, but has little effect on serine-threonine specific kinases, PKC and PKA (IC_{50} >500 μM).[55] As was the case for NXN-6 and Mdm2, a stepwise addition of butein to the A93W CDK2 mutant led to a continuous movement of the newly introduced tryptophan signal (Figure 10). Our experiments show that butein is a weak inhibitor for CDK2 (K_D: 100 ± 50 μM).

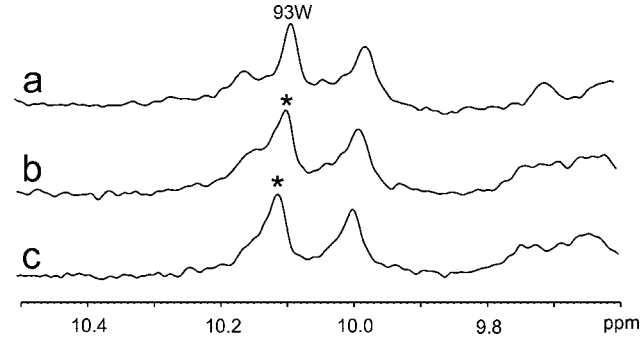

Figure 10. One-dimensional proton NMR spectra of human CDK2−A93W titrated with butein. (a) Unbound CDK2. (b) Molar ratio protein: inhibitor 1:5. (c) Molar ratio protein:inhibitor 1:10. The asterisk indicates the new introduced tryptophan 93W.

Discussion

Our experiments on Mdm2 and CDK2 show that, by introducing Trp residues in surface exposed sites near potential antagonist binding sites, small molecule binding can be monitored through effects on indole proton chemical shifts. We have mutated a total of five residues in human Mdm2 and three residues on CDK2. These mutations change insignificantly protein stability, fold, and binding capabilities. NMR spectra clearly show that side chains of Trp's in the Mdm2 mutants are flexible and get restricted in motions upon binding to p53 (Figure 3 and Supporting Information Figure S3). For example, the tryptophan in the T101W mutant is part of a helix, which goes parallel to the binding pocket for the p53 peptide (Figure 2) and should thus have its side chain pointing outward in the Mdm2 without steric clashes with the rest of the protein. After checking the model of the structure of the Mdm2−T101W mutant, we expected "no danger" that the binding site is altered. Therefore it should bind to ligands in an approximately same way as wt-Mdm2. Indeed, the K_D of binding of p53 (residues 1−73) to the T101W mutant determined by ITC was 0.3 μM, whereas the wt-Mdm2/p53 exhibits K_D of 0.5 μM (Table 1). We also measured the binding of wt-Mdm2 and Mdm2−T101W to the largest available, stable construct of p53 (refs 12, 49), i.e., the domain of p53 that encompasses residues 1−310 of the total of 393 of human p53 (Supporting Information Figure S9). The K_Ds were similar to those of the p53 N-terminal domain only: 0.6 μM and 0.2 μM, for wt-Mdm2 and Mdm2−T101W, respectively.

Two mutants in Mdm2, T101W and K98W, proved to be universal and excellent reporters of all three antagonist−protein and protein−protein interactions we have studied, i.e., the interaction of small molecules with Mdm2, the Mdm2-p53 interaction, and the inhibition of the Mdm2−p53 binding by small-molecular-weight compounds. These two mutants could also provide quantitative characterization of these interactions in the form of K_Ds and fractions of the released p53 or Mdm2 from their mutual binding. For example, recently developed inhibitors of the Mdm2-p53 interaction, compounds called NXN-6 (and NXN-7, data not shown)[50,51] bind to Mdm2 with K_D′s of ca. 5 μM, and our data shows that they are less potent than nutlins in dissociating the Mdm2−p53 complex. For CDK2, the A93W mutant gave the best results in distinguishing between strong and weak binders. The H84W mutant gave similar results, the overlapping of the introduced tryptophan signal with one of the four naturally present tryptophan signals required, however, a little bit more careful analysis of the binding data. The detection of strong and weak binders by introduction of tryptophans to the CDK2 sequence, a protein which already has four tryptophans in the sequence, shows that the method could be expanded to larger proteins, which are expected to have many natural tryptophans. Even coincidental overlap with a naturally present tryptophan signal is not detrimental.

In some cases, the naturally present tryptophans might be used for detecting the binding without the need of introducing extra tryptophans. This is the case when tryptophans actively participate in the binding to ligands or are close enough to the binding pocket and are therefore sensitive in NMR experiments. This is illustrated by the titration of the protein MAD2 with MAD1 or CDC20 peptides (Supporting Information Figures S7 and S8).

In principle, one can use any 1D resolved signals of proteins, including backbone amides and methyl groups, to detect ligand binding. In most practical cases, however, it is not possible to use amide and methyl signals for proteins larger than ca. 10 kDa because these signals are not resolved in 1D proton NMR spectra and/or might not be sensitive to ligand addition. For

example, CDK2 gave clear spectra in the methyl region (Supporting Information Figures S4a and S4b). However, the movement of NMR peaks is so complicated that no unambiguous conclusion can be reached from the data. Small molecule binding is usually in a μM range, and a large excess of these compounds must be used to observe the binding to the protein (binary interactions) or inhibition of the protein−protein interaction (NMR competition experiments on ligand−protein complexes). The signals of a compound obscure usually the signals from a protein. This gets worse if we use mixtures of compounds. In addition, several compounds for Mdm2 required 0.3% of detergents for solubilization. These types of detergents (Tween 20, CHAPS) totally obscured aliphatic NMR signals of Mdm2.

We have used both a naturally occurring Trp of p53 and a non-native Trp of Mdm2 for the 1D AIDA-NMR monitoring of the p53−Mdm2 complex. Because the highly flexible nature of the N-terminal domain of p53 is specific to this domain,[12,13,49] only tryptophan mutants of Mdm2 can serve as universal reporters. For a specific case of the p53-Mdm2 interaction, we can now monitor directly the status of the Mdm2 binding to p53 and the p53 binding to Mdm2 and what happens to these two proteins upon addition of potential antagonists. Supporting Information Figures S10 and S11 show an example of a compound that releases the folded p53; however, no Trp signal of Mdm2 is seen, thus indicating that the dissociation of the p53-Mdm2 complex is through the denaturation of Mdm2 as no protein precipitation was observed. AIDA provides thus unambiguous information on how an antagonist of a protein−protein interaction is capable to dissociate the complex. It is noteworthy to point out that the dissociation is detected irrespective of the protein the compound acts upon; thus, both targets are checked simultaneously and the detection of the binding site and the inhibition strength is obtained, in principle, without any prior knowledge of these parameters. This approach therefore targets protein−protein interactions and not a single protein.

Because AIDA-NMR is a competition assay, it is possible to determine the K_D of the inhibitor−protein affinity from a single experiment (Table 1).[13] For the Mdm2−p53 interaction, the definitions of dissociation constants are as follows: K_D^C = [Mdm2] [p53]/([p53−Mdm2], for the reaction: Mdm2 + p53 = Mdm2−p53, and K_D^I = [Mdm2][antagonist]/([Mdm2−antagonist] for Mdm2 + antagonist = Mdm2−antagonist. Partial recovery of the reporter protein in NMR spectra has to be quantitatively determined (i.e., [Mdm2] or [p53]), and knowing the strength of the protein−protein interaction (K_D^C), total concentrations of the ligand, and proteins ($[Mdm2]_{total}$, $[p53]_{total}$ $[antagonist]_{total}$), we can obtain the strength of the ligand−protein binding (K_D^I).[13] Accuracy of this determination crucially depends on the sensitivity of the NMR spectrum. For a 2D version of AIDA-NMR, we found in our practice that 30% of the dissociated Mdm2 is required for a clear-cut detection by ^{15}N HSQCs (using ca. 0.1 mM concentrations of protein complexes).[13] For the 1D proton Trp version, the detection threshold is lower and the accuracy of integrating the fraction of recovered NMR signals higher, thus allowing the reliable K_D determination with a cutoff of dissociation of 8% and protein concentrations as low as 10 μM (for a ca. 3 h experiment in a 5 mm NMR tube, Supporting Information Figure S12).

The method described here can be used for many proteins. The design of point mutations needs structural information for a protein of interest, which is however in most cases available. Our method can easily be combined with 2D NMR methods that use labeled proteins. For example, we use our Trp mutants ^{15}N labeled in the every day practice, putting up with a small inconvenience of the NH splitting of Trp indole signals. There is of course a tradeoff of the speed and spectral simplicity of our method for a complete coverage of NMR signals of a protein obtained with 2D ^{15}N−^{1}H-correlation NMR spectroscopy. Thus, mapping binding interfaces in proteins is best achieved with the 2D NMR and ^{15}N(^{13}C) labeled proteins. This can be achieved with the "traditional" SAR by NMR[1−8] or using a recently devised, elegant assay, IDIS-NMR, which allows for simultaneous 2D NMR monitoring of two protein components of the complex in a single sample.[56]

2D NMR-based "SAR-by-NMR" approaches that employ ^{15}N-labeled proteins typically several hours per one spectrum. With our method, we could cut this time to several minutes. For example, an average NMR experiment with Mdm2 mutants took 8 min to obtain a 1D spectrum with 128 scans with reasonable S/N. A four-step titration can be recorded in 30 min. For comparison, an average ^{1}H−^{15}N HSQC spectrum have taken 5 h (128 scans, 96 increments)[12,13] for Mdm2 samples of the same concentration as that used in the 1D experiment. We thus believe that our technology can potentially reform the process of NMR-based screening for lead compounds, allowing for high-throughput screening pipelines. It should also allow analysis of proteins from low-yield protein production systems such as cell-free, insect cell, and other eukaryotic expression hosts. Importantly, the method provides also a rapid and straightforward quantitative characterization of the antagonist−protein and antagonist−protein−protein interactions in the form of K_Ds and fractions of the released proteins from their mutual bindings. The features of our technologies described here should thus have useful applications in lead generation in drug discovery.

Experimental Section

Protein Expression and Purification. The recombinant human Mdm2 mutants (residues 1−118) were obtained from an *Escherichia coli* BL21(DE3) RIL expression system using the pET−46Ek/LIC vector. Cells were grown at 37 °C and induced with 1 mM IPTG at an OD_{600nm} of 0.7. The T47W and T63W mutants were expressed for 3 h at 37 °C and purified from inclusion bodies, refolded, and further purified by Buthy-Sepharose FF (Amersham). All other mutants were expressed for 12 h at 20 °C and were first purified under native condition using Ni-NT Agarose (Qiagen). The final purification of all proteins was by HiLoad 16/60 Superdex75 gel filtration (Pharmacia). p53 (residues-73) was expressed as a GST-fusion protein and purified by gel filtration on glutathione sepharose (GE Healthcare) and HiLoad 16/60 Superdex75 (Pharmacia). Complexes were made by mixing p53 and Mdm2 in a ratio of 1:2. The excess of Mdm2 was then removed by gel filtration. The recombinant human CDK2 mutants (residues 1−298) were obtained from an *E. coli* BL21(DE3) RIL expression system using the pET-28 vector. Cells were grown at 37 °C and induced with 1 mM IPTG at an OD_{600nm} of 0.7. All mutants were expressed for 12 h at 20 °C and were first purified under native condition using Ni-NT agarose (Qiagen). The final purification of all proteins was by the HiLoad 16/60 Superdex75 gel filtration (Amersham Biosciences).

NMR Methods. All NMR spectra were acquired at 300 K on a Bruker DRX 600 MHz spectrometer equipped with a cryoprobe except for the MAD2 titration, which was carried out on a Bruker DRX 500 MHz spectrometer. Typically, NMR samples contained up to 0.1 mM of protein in 50 mM KH_2PO_4, 50 mM Na_2HPO_4, 150 mM NaCl, 5 mM DTT, pH 7.4. Water suppression was carried out using the WATERGATE sequence. NMR data were processed using the Bruker program Xwin-NMR version 3.5. NMR ligand binding experiments were carried out in an analogous way to those

previously described.[27] Five hundred mL of the protein sample containing 10% D_2O, at a concentration of about 0.1 mM, and a 20 mM stock solution of nutin-3 (purchased from Cayman Chemical, MI) or 20 mM NXN-6 (NexusPharma) in DMSO-d_6 were used in all of the experiments. The maximum concentration of DMSO at the end of titration experiments was less than 1%. The pH was maintained constant during the entire titration.

Isothermal Titration Calorimetry (ITC). The binding of GST-p53 (residues 1−73) and p53 (residues 1−310) constructs to Mdm2 (residues 1−118) wild type and mutants was measured by isothermal titration calorimetry using a VP-ITC MicroCalorimeter (MicroCal, Northampton, MA). The protein concentration in the reservoir solution was around 0.02−0.03 mM, the concentration of the titrant was around 0.2−0.3 mM. Measurements were carried out in PBS, 2 mM TCEP, pH 7.4). All steps of the data analysis were performed using ORIGIN (V5.0) software provided by the manufacturer.

Acknowledgment. We thank Dr. Mahavir Singh and Jolanta Ciombor for fruitful discussion.

Supporting Information Available: Additional AIDA experiment with the F55W mutant, titration of MAD2 with MAD1 peptide, ITC experiments, thermal shift assays, complete 1D-NMR spectra of wt-protein and mutants. This material is available free of charge via the Internet at http://pubs.acs.org.

References

(1) Shuker, S. B.; Hajduk, P. J.; Meadows, R. P.; Fesik, S. W. Discovering high-affinity ligands for proteins: SAR by NMR. *Science* **1996**, *274*, 1531–1534.
(2) Stockman, B. J.; Dalvit, C. NMR screening techniques in drug discovery and drug design. *Prog. NMR Spectrosc.* **2002**, *41*, 187–231.
(3) Jahnke, W.; Widmer, H. Protein NMR in biomedical research. *Cell. Mol. Life Sci.* **2004**, *61*, 580–599.
(4) Lepre, C. A.; Moore, J. M.; Peng, J. W. Theory and applications of NMR-based screening in pharmaceutical research. *Chem. Rev.* **2004**, *104*, 3641–3676.
(5) Peng, J. W.; Moore, J.; Abdul-Manan, N. NMR experiments for lead generation in drug discovery. *Prog. NMR Spectrosc.* **2004**, *44*, 225–256.
(6) Klages, J.; Coles, M.; Kessler, H. NMR-based screening: a powerful tool in fragment-based drug discovery. *Mol. Biosystems* **2006**, *2*, 319–331.
(7) Prestegard, J. H.; Valafar, H.; Glushka, J.; Tian, F. Nuclear Magnetic Resonance in the era of structural genomics. *Biochemistry* **2001**, *40*, 8677–8685.
(8) Meyer, B.; Peters, T. NMR spectroscopy techniques for screening and identifying ligand binding to protein receptors. *Angew. Chem., Int. Ed.* **2003**, *42*, 864–90.
(9) Aramini, J. M.; Rossi, P.; Anklin, C.; Rong Xiao, R.; Montelione, G. T. Microgram-scale protein structure determination by NMR. *Nature Methods* **2007**, *6*, 491–493.
(10) Buehler, C.; Dreessen, J.; Mueller, K.; So, P. T.; Schilb, A.; Hassiepen, U.; Stoeckli, K. A.; Auer, M. Multiphoton excitation of intrinsic protein fluorescence and its application to pharmaceutical drug screening. *Assay Drug Dev. Technol.* **2005**, *3*, 155–167.
(11) Wüthrich, K. *NMR of Proteins and Nucleic Acids*; Wiley: New York, 1986.
(12) D'Silva, L.; Ozdowy, P.; Krajewski, M.; Rothweiler, U.; Singh, M.; Holak, T. A. Monitoring the effects of antagonists on protein−protein interactions with NMR spectroscopy. *J. Am. Chem. Soc.* **2005**, *127*, 13220–13226.
(13) Krajewski, M.; Rothweiler, U.; D'Silva, L.; Majumdar, S.; Klein, C.; Holak, T. A. An NMR-based antagonist induced dissociation assay for targeting the ligand−protein and protein−protein interactions in competition binding experiments. *J. Med. Chem.* **2007**, *50*, 4382–4387.
(14) Vousden, K. H.; Lane, D. P. p53 in health and disease. *Nature Rev. Mol. Cell Biol.* **2007**, *8*, 275–283.
(15) Vassilev, L. T. MDM2 inhibitors for cancer therapy. *Trends Mol. Med.* **2006**, *13*, 23–31.
(16) Chene, P. Inhibiting the p53−MDM2 interaction: an important target for cancer therapy. *Nat. Rev. Cancer* **2003**, *3*, 102–109.
(17) Chen, J.; Marechal, V.; Levine, A. J. Mapping of the p53 and MDM-2 interaction domains. *Mol. Cell. Biol.* **1993**, *13*, 4107–4114.
(18) Picksley, S. M.; Vojtesek, B.; Sparks, A.; Lane, D. P. Immunochemical analysis of the interaction of p53 with MDM2; fine mapping of the MDM2 binding site on p53 using synthetic peptides. *Oncogene* **1994**, *9*, 2523–2529.
(19) Böttger, V.; Böttger, A.; Howard, S. F.; Picksley, S. M.; Chene, P.; Garcia.Echeverria, C.; Hochkeppel, H. K.; Lane, D. P. Identification of novel MDM2 binding peptides by phage display. *Oncogene* **1996**, *13*, 2141–2147.
(20) Böttger, A.; Böttger, V.; Sparks, A.; Liu, W. L.; Howard, S. F.; Lane, D. P. Design of a synthetic MDM2-binding miniprotein that activates the p53 response in vivo. *Curr. Biol.* **1997**, *7*, 860–869.
(21) Schon, O.; Friedler, A.; Bycroft, M.; Freund, S. M. V.; Fersht, A. R. Molecular mechanism of the interaction between MDM2 and p53. *J. Mol. Biol.* **2002**, *323*, 491–501.
(22) Schon, O.; Friedler, A.; Freund, S.; Fersht, A. R. Binding of p53-derived ligands to MDM2 induces a variety of long range conformational changes. *J. Mol. Biol.* **2004**, *336*, 197–202.
(23) Martins, C. P.; Brown-Swigart, L.; Evan, G. I. Modeling the therapeutic efficacy of p53 restoration in tumors. *Cell* **2006**, *127*, 1323–1334.
(24) Xue, W.; Zender, L.; Miething, C.; Dickins, R. A.; Hernando, E.; Krizhanovsky, V.; Cordon-Cardo, C.; Lowe, S. W. Senescence and tumour clearance is triggered by p53 restoration in murine liver carcinomas. *Nature* **2007**, *44*, 656–660.
(25) Ventura, A.; Kirsch, D. G.; McLaughlin, M. E.; Tuveson, D. A.; Grimm, J.; Lintault, L.; Newman, J.; Reczek, E. E.; Weissleder, R.; Jacks, T. Restoration of p53 function leads to tumour regression in vivo. *Nature* **2007**, *445*, 661–665.
(26) Vassilev, L. T.; Vu, B. T.; Graves, B.; Carvajal, D.; Podlaski, F.; Filipovic, Z.; Kong, N.; Kammlott, U.; Lukacs, C.; Klein, C.; Fotouhi, N.; Liu, E. A. In vivo activation of the p53 pathway by small-molecule antagonists of MDM2. *Science* **2004**, *303*, 844–848.
(27) Stoll, R.; Renner, C.; Hansen, S.; Palme, S.; Klein, C.; Belling, A.; Zeslawski, W.; Kamionka, M.; Rehm, T.; Muhlhahn, P.; Schumacher, R.; Hesse, F.; Kaluza, B.; Voelter, W.; Engh, R. A.; Holak, T. A. Chalcone derivatives antagonize interactions between the human oncoprotein MDM2 and p53. *Biochemistry* **2001**, *40*, 336–344.
(28) Murray, J. K.; Gellman, S. H. Targeting protein−protein interactions: lessons from p53/MDM2. *Biopolymers.* **2007**, *88*, 657–686.
(29) Dey, A.; Verma, C. S.; Lane, D. P. Updates on p53: modulation of p53 degradationas a therapeutic approach. *Br. J. Cancer* **2008**, *984*, 4–8.
(30) Grasberger, B. L.; Lu, T.; Schubert, C.; Parks, D. J.; Carver, T. E.; Koblish, H. K.; Cummings, M. D.; LaFrance, L. V.; Milkiewicz, K. L.; Calvo, R. R.; Maguire, D.; Lattanze, J.; Franks, C. F.; Zhao, S.; Ramachandren, K.; Bylebyl, G. R.; Zhang, M.; Manthey, C. L.; Petrella, E. C.; Pantoliano, M. W.; Deckman, I. C.; Spurlino, J. C.; Maroney, A. C.; Tomczuk, B. E.; Molloy, C. J.; Bone, R. F. Discovery and cocrystal structure of benzodiazepinedione HDM2 antagonists that activate p53 in cells. *J. Med. Chem.* **2005**, *48*, 909–912.
(31) Shangary, S.; Qin, D. G.; McEachern, D.; Liu, M. L.; Miller, R. S.; Qiu, S.; Nikolovska-Coleska, Z.; Ding, K.; Wang, G. P.; Chen, J. Y.; Bernard, D.; Zhang, J.; Lu, Y. P.; Gu, Q. Y.; Shah, R. B.; Pienta, K. J.; Ling, X. L.; Kang, S. M.; Guo, M.; Sun, Y.; Yang, D. J.; Wang, S. M. Temporal activation of p53 by a specific MDM2 inhibitor is selectively toxic to tumors and leads to complete tumor growth inhibition. *Proc. Natl. Acad. Sci. U.S.A.* **2008**, *105*, 3933–3938.
(32) Dey, A.; Verma, C. S.; Lane, D. P. Updates on p53: modulation of p53 degradatioasatherapeutic approach. *Br. J. Cancer* **2008**, *98*, 4–8.
(33) Cohen, P. Protein kinases, the major drug targets of the 21st century. *Nat. Rev. Drug Discovery* **2002**, *1*, 309–316.
(34) Knockaert, M.; Greengard, P.; Meijer, L. Pharmacological inhibitors of cyclin-dependent kinases. *Trends Pharmacol. Sci.* **2002**, *23*, 417–425.
(35) DeGregori, J.; Leone, G.; Ohtani, K.; Miron, A.; Nevins, J. R. E2F1 accumulation bypasses a G1 arrest resulting from the inhibition of G1 cyclin-dependent kinase activity. *Genes Dev.* **1995**, *9*, 2873–2887.
(36) Arata, Y.; Fujita, M.; Ohtani, K.; Kijima, S.; Kato, J. Y. Cdk2-dependent and -independent pathways in E2F-mediated **S** phase induction. *J. Biol. Chem.* **2000**, *275*, 6337–6345.
(37) Sherr, C. J. Cancer cell cycles. *Science* **1996**, *274*, 1672–1677.
(38) Lukas, J.; Parry, D.; Aagaard, L.; Mann, D. J.; Bartkova, J.; Strauss, M.; Peters, G.; Bartek, J. etinoblastoma-protein-dependent cell-cycle inhibition by the tumour suppressor p16. *Nature* **1995**, *375*, 503–506.
(39) Lundberg, A. S.; Weinberg, R. A. Functional inactivation of the retinoblastoma protein requires sequential modification by at least two distinct cyclin−cdk complexes. *Mol. Cell. Biol.* **1998**, *18*, 753–761.
(40) Shapiro, G. I. Cyclin-dependent kinase pathways as targets for cancer treatment. *J. Clin. Oncol* **2006**, *24*, 1770–1783.
(41) Huwe, A.; Mazitschek, R.; Giannis, A. Small molecules as inhibitors of cyclin-dependent kinases. *Angew. Chem., Int. Ed.* **2003**, *42*, 2122–2138.
(42) Meijer, L.; Raymond, E. Roscovitine and Other Purines as Kinase Inhibitors. From Starfish Oocytes to Clinical Trials. *Acc. Chem. Res.* **2003**, *36*, 417–425.

(43) Meijer, L.; Borgne, A.; Mulner, O.; Chong, J. P.; Blow, J. J.; Inagaki, N.; Inagaki, M.; Delcros, J. G.; Moulinoux, J. P. Biochemical and cellular effects of roscovitine, a potent and selective inhibitor of the cyclin-dependent kinases cdc2, cdk2, and cdk5. *Eur. J. Biochem.* **1997**, *243*, 527–536.

(44) Whittaker, S. R.; Walton, M. I.; Garrett, M. D.; Workman, P. The cyclin-dependent kinase inhibitor CYC202 (R-roscovitine) inhibits retinoblastoma protein phosphorylation, causes loss of cyclin D1 and activates the mitogen.activated protein kinase pathway. *Cancer Res.* **2004**, *64*, 262–272.

(45) McClue, S. J.; Blake, D.; Clarke, R.; Cowan, A.; Cummings, L.; Fischer, P. M.; MacKenzie, M.; Melville, J.; Stewart, K.; Wang, S.; Zhelev, N.; Zheleva, D.; Lane, D. P. In vitro and in vivo antitumor properties of the cyclin dependent kinase inhibitor CYC202 (R-roscovitine). *Int. J. Cancer* **2002**, *102*, 463–468.

(46) Raynaud, F. I.; Whittaker, S. R.; Fischer, P. M.; McClue, S.; Walton, M. I.; Barrie, S. E.; Garrett, M. D.; Rogers, P.; Clarke, S. J.; Kelland, L. R.; Valenti, M.; Brunton, L.; Eccles, S.; Lane, D. P.; Workman, P. In vitro and in vivo pharmacokinetic−pharmacodynamic relationships for the trisubstituted aminopurine cyclin-dependent kinase inhibitors olomoucine, bohemine and CYC202. *Clin. Cancer Res.* **2005**, *11*, 4875–4887.

(47) Benson, C.; White, J.; De Bono, J.; O'Donnell, A.; Raynaud, F.; Cruickshank, C.; McGrath, H.; Walton, M.; Workman, P.; Kaye, S.; Cassidy, J.; Gianella-Borradori, A.; Judson, I.; Twelves, C. A phase I trial of the selective oral cylin-dependent kinase inhibitor seliciclib (CYC202, R-roscovitine) administered twice daily for 7 days every 21 days. *Br. J. Cancer* **2007**, *96*, 29–37.

(48) Kussie, P. H.; Gorina, S.; Marechal, V.; Elenbaas, B.; Moreau, J.; Levine, A. J.; Pavletich, N. P. Structure of the MDM2 oncoprotein bound to the p53 tumor supressor transcativation domain. *Science* **1996**, *274*, 948–953.

(49) Dawson, R.; Mueller, L.; Dehner, A.; Klein, C.; Kessler, H.; Buchner, J. The N-terminal domain of p53 is natively unfolded. *J. Mol. Biol.* **2003**, *332*, 1131–1141.

(50) Weber, L. Tetrahydro-isoquinolin-1-ones for the treatment of cancer. International Patent PCT/EP2006/002471, 2006.

(51) Rothweiler, U.; Czarna, A.; Krajewski, M.; Ciombor, J.; Kalinski, C.; Khazak, V.; Ross, G.; Skobeleva, N.; Weber, L.; Holak, T. A. Isoquinolin-1-one Inhibitors for the MDM2−p53 Interaction. *ChemMedChem* **2008**, *3*, 1118–1128.

(52) Laurie, N. A.; Donovan, S. L.; Shih, C. S.; Zhang, J.; Mills, N.; Fuller, C.; Teunisse, A.; Lam, S.; Ramos, Y.; Mohan, A.; Johnson, D.; Wilson, M.; Rodriguez-Galindo, C.; Quarto, M.; Francoz, S.; Mendrysa, S. M.; Guy, R. K.; Marine, J. C.; Jochemsen, A. G.; Dyer, M. A. Inactivation of the p53 pathway in retinoblastoma. *Nature* **2006**, *444*, 61–66.

(53) Jeffrey, P. D.; Russo, A. A.; Polyak, K.; Gibbs, E.; Hurwitz, J.; Massague, J.; Pavletich, N. P. Mechanism of CDK activation revealed by the structure of a cyclin A−CDK2 complex. *Nature* **1995**, *376*, 313–320.

(54) Yu, S. M.; Cheng, Z. J.; Kuo, S. C. Endothelium-dependent relaxation of rat aorta by butein, a novel cyclic AMP-specific phosphodiesterase inhibitor. *Eur. J. Pharmacol.* **1995**, *280*, 69–77.

(55) Yang, E.; Zhang, K.; Li Cheng, Y.; Mack, P. Butein, a Specific Protein Tyrosine Kinase Inhibitor. *Biochem. Biophys. Res. Commun.* **1998**, *245*, 435–438.

(56) Golovanov, A. P.; Blankley, R. T.; Avis, J. M.; Bermel, W. Isotopically discriminated NMR spectroscopy: A tool for investigating complex protein interactions in vitro. *J. Am. Chem. Soc.* **2007**, *129*, 6528–6535.

JM8002813